ASIAN JOURNAL OF ORGANIC CHEMISTRY

www.AsianJOC.org

A Journal of

ACES
Asian Chemical Editorial Society

REPRINT

WILEY-VCH

ACES Asian Chemical Editorial Society

DOI: 10.1002/ajoc.202000432

ASIAN JOURNAL OF ORGANIC CHEMISTRY
Full Paper

Experimental and Computational Study on the Reaction Pathways of Diradical Intermediates Formed from Myers-Saito Cyclization of Maleimide-Based Enediynes

Haotian Lu, Mengsi Zhang, Baojun Li, Hailong Ma, Wenbo Wang, Yun Ding, Xinxin Li,* and Aiguo Hu*[a]

Abstract: Great efforts have been dedicated to studying the thermal-induced Myers-Saito cyclization (MSC) of enyne-allene as the resulting diradicals hold significant potential in various fields, especially in antitumor applications. Besides abstracting hydrogen from DNA backbone and further inducing tumor cell death, the diradicals might react through multiple pathways and lose their efficiency in antitumor applications. The in-depth understanding of the reaction pattern of these highly reactive diradical intermediates will provide clear guidelines for the design of new enyne-allene with high antitumor potency. Herein, we report detailed studies to reveal the reaction mechanism of ketal-conjugated enediynes, which are hydrolyzed and tautomerized into enyne-allene structures in acidic condition and produce diradicals through MSC. Further 1,3-hydrogen atom transfer (HAT)/6-endo cyclization to yield pyran-type product or 5-endo cyclization/1,4-HAT to yield furan-type product were confirmed and rationalized through computational studies. The proposed reaction pathways were further verified with deuterium labeling experiments. Based on these new findings, a new enediyne with asymmetric structure and tertbutyl group to block the HAT process was synthesized, which demonstrated much higher cytotoxicity against the HeLa cell line with a half inhibition concentration (IC_{50} value) down to submicromolar level.

Introduction

Since the first elucidation of the cyclization mechanism of natural enediyne Neocarzinostatin,[1] the highly reactive enyne-allene structures have attracted tremendous attentions.[2] In physiological environment, the enediyne core structure of Neocarzinostatin transforms into enyne-allene structure and undergoes Myers-Saito cyclization (MSC) to generate diradical intermediate that is capable of abstracting hydrogen from DNA backbone and further inducing cell death.[3] Besides abstracting hydrogen intermolecularly, the two carbon radical centers generated from MSC may react through multiple pathways.[4] A variety of interesting work has demonstrated the diversified fates of diradical intermediate.[5] Wang et al. showed that the more reactive phenyl radical of the diradical intermediate underwent a five- or six-membered ring cyclization (depending on the structure of enyne-allene) to produce a relative stable radical, which was trapped with the benzyl radical through subsequent hydrogen atom transfer (HAT) to form carbon-carbon double bond or new aromatic ring.[6] In the report by Finn et al.,[7] the diradical intermediates reacted with each other to form dimeric product or underwent cyclopropane ring opening reaction and further abstracted hydrogens from 1,4-cyclohexadiene. Studies that incorporating *in situ* propargyl-allene tautomerization to form enyne-allene from enediyne, followed by MSC and subsequent radical reaction (described as tandem MSC) have also been reported.[5b,g,8] Base and metal complex are typically applied to facilitate the propargyl-allene tautomerization. Shibuya et al. designed enediyne systems conjugated with malonyl ester groups, which hydrolyzed under basic conditions to form enyne-allenes and further underwent thermal-induced MSC.[9] In the works by Hashmi[10] and Yang,[11] detailed experimental and theoretical studies were conducted to demonstrate the mechanism of organometallic Au(I) complex catalyzed enediyne transformation and the subsequent tandem MSC reactions.

The in-depth understanding of the reaction pathways of enediyne, with no doubt, will provide clear guidelines for the design of new enediyne to improve their performance in various fields. Our group has been dedicated to design and study maleimide-based enediynes for antitumor applications.[12] Recently, we uncovered a new mechanism named as maleimide-assisted rearrangement and cycloaromatization (MARACA) to trigger the antitumor activity of acyclic enediynes through the facilitated tautomerization of enediyne to enyne-allene and the generation of radical species under physiological conditions.[13] We also found that the phenyl radical formed from MSC could underwent 5-endo ring closure to form a stable product, suggesting the presence of different pathways of the diradical intermediates beside hydrogen-abstracting reactions. Along the same line, we designed enediyne **1** with acid-labile protecting groups which could be converted to enyne-allene **2** and **3** in the present of trifluoroacetic acid (TFA) at 0 °C

[a] H. Lu, M. Zhang, B. Li, H. Ma, W. Wang, Dr. Y. Ding, Prof. Dr. X. Li, Prof. Dr. A. Hu
Shanghai Key Laboratory of Advanced Polymeric Materials, School of Materials Science and Engineering
East China University of Science and Technology
Shanghai 200237 (P. R. China)
E-mail: xinxinli@ecust.edu.cn
hagmhsn@ecust.edu.cn

Supporting information for this article is available on the WWW under https://doi.org/10.1002/ajoc.202000432

(Scheme 1). The highly reactive enyne-allenes further underwent MSC to generate radical species at 37 °C, endowing them high antitumor activity comparable to many commercial antitumor agents.[14]

To optimize the molecular design of these maleimide-based enediynes to further boost their antitumor potency, the reaction pattern of the diradical intermediate was investigated in this work. Two kinds of stable compounds were isolated from the reaction mixture of enediyne **1** and they were identified to consist pyran-type and furan-type structures. Based on the identified products of enediyne **1**, we proposed reaction pathways for enediyne **1**, including thermal-induced MSC, radical-induced cyclization and HAT process. Computational calculations and deuterium labeling experiments were conducted to verify the proposed reaction pathways. With this finding as the guideline, a new enediyne was designed and synthesized, which demonstrated much higher cytotoxicity against HeLa cell line than enediyne **1** with half inhibition concentration (IC_{50} value) down to submicromolar level.

Results and Discussion

Direct hydrolysis and thermal reaction of enediyne **1** was conducted in the presence of TFA at room temperature for 24 h (Scheme 2A). After complete conversion of the starting material, three small molecular products were separated out and identified, where the pyran-type products **4** and **5** were isolated with the yields of 7% and 11% respectively, and the furan-type product **6** was isolated as the major product with a yield of 42%. The structure of **6** was identified by high resolution mass spectroscopy (HRMS), nuclear magnetic resonance (NMR, ^{1}H, ^{13}C), distortionless enhancement by polarization transfer (DEPT), heteronuclear single quantum correlation (HSQC), and heteronuclear multiple bond correlation (HMBC) spectroscopies (shown in SI Figure S6–S8). The structures of pyran-type products **4** and **5** were also verified by ^{1}H, ^{13}C NMR and HRMS analysis (SI).

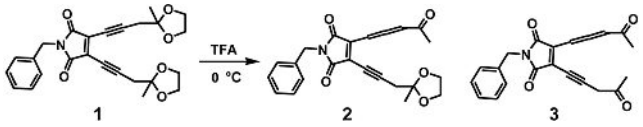

Scheme 1. Hydrolysis of enediyne **1** at 0°C.

The disappearance of the methylene signals of the ketal groups in the ^{1}H NMR spectrum of **6** (Figure S6) suggests that two carbonyl groups are completely deprotected. However, there is only one peak at 203.9 ppm corresponding to free carbonyl group in the ^{13}C NMR spectrum, implying the reaction of one of the carbonyl groups. The peaks at 2.19 and 6.48 ppm with integration ratio of 1:3 are similar to the structure of 2-methylbenzofuran,[15] suggesting the occurrence of intramolecular ring closure. The presence of benzofuran moiety in compound **6** is unambiguously confirmed with HSQC and HMBC spectroscopy (Scheme 2B) analysis. The signals of (H_4,C_7), (H_4,C_9), and (H_4,C_{10}) in HMBC as well as the signal of (H_4,C_8) in HSQC establish the connection of C_{10}–C_7–C_8–C_9, verifying the existence of furan ring. While the relation of C_4–C_5–C_6–C_{14} is confirmed by the correlation of H_3, the linkage of C_7-C_8-C_9-C_{13} is proved by the correlation of H_5. Importantly, C_7 gives the signals with H_2, H_3, H_4, and H_5 in HSQC, further confirming the configuration of 2-methylbenzofuran.

Verified radical involvement in the reaction[16] (SI Figure S1), we proposed the reaction pathways for the formation of those products, which involved thermal MSC, radical-induced cyclization and HATs. The three proposed reaction pathways are depicted in Figure 1. After the hydrolysis of enediyne **1**, two enyne-allene structures (**2** and **3**) are formed[14] and the reaction pathway diverges into pathway A to form compound **4** and

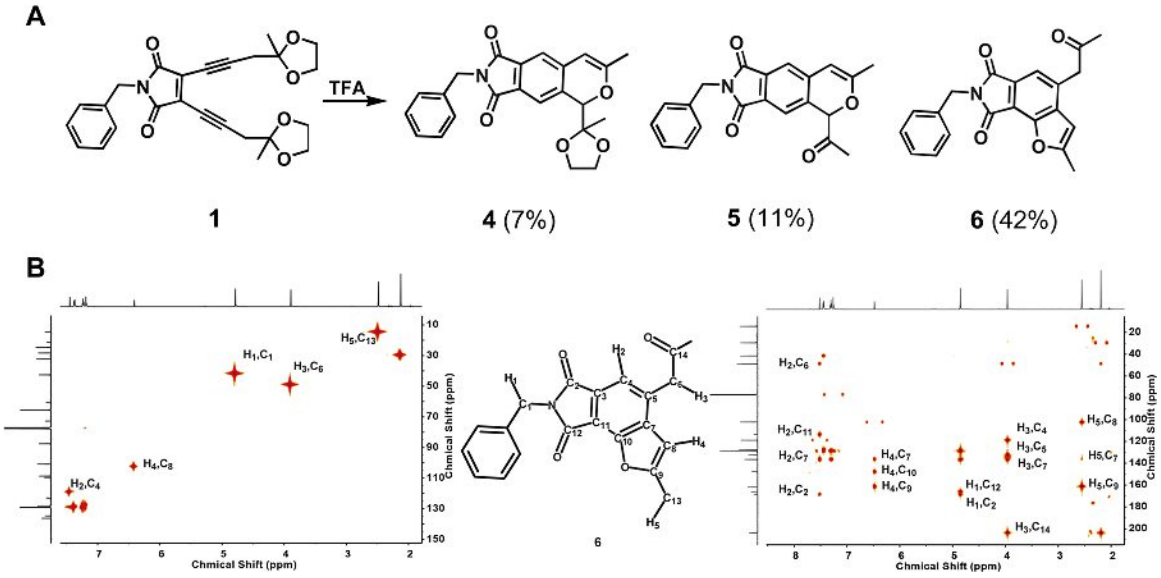

Scheme 2. (A) Schematic illustration of the reaction of enediyne **1** at room temperature in the presence of TFA. (B) HSQC (left) and HMBC (right) spectra of compound **6**.

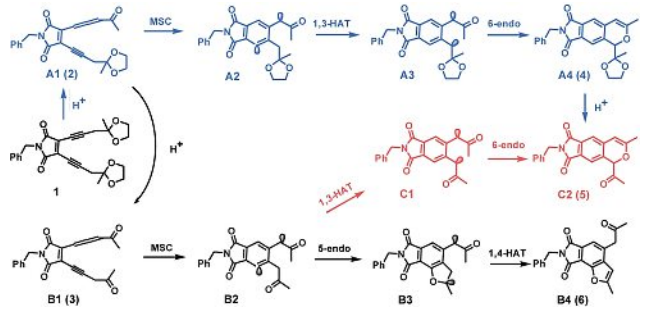

Figure 1. The proposed reaction pathways. Pathway A: blue; pathway B: black; pathway C: red.

pathway B to form compound **6**. For pathway A, the enyne-allene **A1** (**2**) undergoes MSC to form diradical intermediate **A2**. Through a 1,3-HAT, the phenyl radical in **A2** is transformed into a more stable benzyl radical to produce **A3**. With a suitable position, the formed benzyl radical attacks the oxygen atom of carbonyl group to generate **A4** (6-endo cyclization), in which the carbon-oxygen double bond opened and formed the carbon-carbon double bond with the adjacent benzyl radical. As for pathway B, after MSC, the formed phenyl radical **B2** attacks the neighboring oxygen atom of carbonyl to form **B3** through 5-endo cyclization. Next, an unusual 1,4-HAT[17] happens to **B3** and the two radicals are trapped in the carbon-carbon double bond resulting in **B4** (compound **6**). While the compound **5** could be the product of **4** through deprotection of ketal group for the first guess, we consider that structure **5** could also yield through pathway C which is the same as pathway A except carbonyl groups are all deprotected.

To verify the proposed reaction pathways, density functional theory (DFT) calculations was performed in GAUSSIAN09 program[18] at the (U)B3LYP/6-31G(d) level with Grimme's D3 dispersion correction.[19] The reactants were chosen to be **AI** and **BI** in Figure 2 (similar to compound **2** and **3** albeit with the benzyl group at the maleimide moiety being replaced with methyl group to reduce calculation burden). The previous reports from our group and other groups had demonstrated that such a computational setup was suitable for enediyne systems.[8f,13–14,20] Unrestricted DFT method together with broken symmetry ansatz was employed in the structure optimizations of transition states in MSC and the resulted diradical products. It turned out that only the diradicals have the open shell characteristic. Harmonic vibration frequency calculations were carried out at 298.15 K and the optimized structures are all shown to be either minima (with no imaginary frequency) or transition states (with only one imaginary frequency). Further intrinsic reaction coordinate calculations confirmed that all the transition states correspond to the reactions of our interest. The calculations were chosen to be run in gas phase as the solvent effect have negligible influence on the energy profile (the calculations of pathway A were run in both gas and solvent phase to show the differences, SI Table S1, S2).

The calculated reaction pathways and the optimized structures of transition states are shown in Figure 2 and Figure 3. The singlet-triplet splitting for the diradical intermediates are shown in Table S3. The singlets were all lower in energy except in one case demonstrating a small difference (**BIII**) and therefore singlet states were used in determining the free energy profile. Both pathway A and B are initiated with MSC to form diradical intermediate **AII** and **BII** via the transition states **ATSI** and **BTSI** with the activation energy of 24.5 and 27.5 kcal/mol respectively. The absolute MSC energy barriers for AI and BI are in the range of previous reported MSC energy barriers of related compounds (from 20 to 30 kcal/mol).[8f,21] While the diradical intermediate **AII** further results in **AIV** through tandem

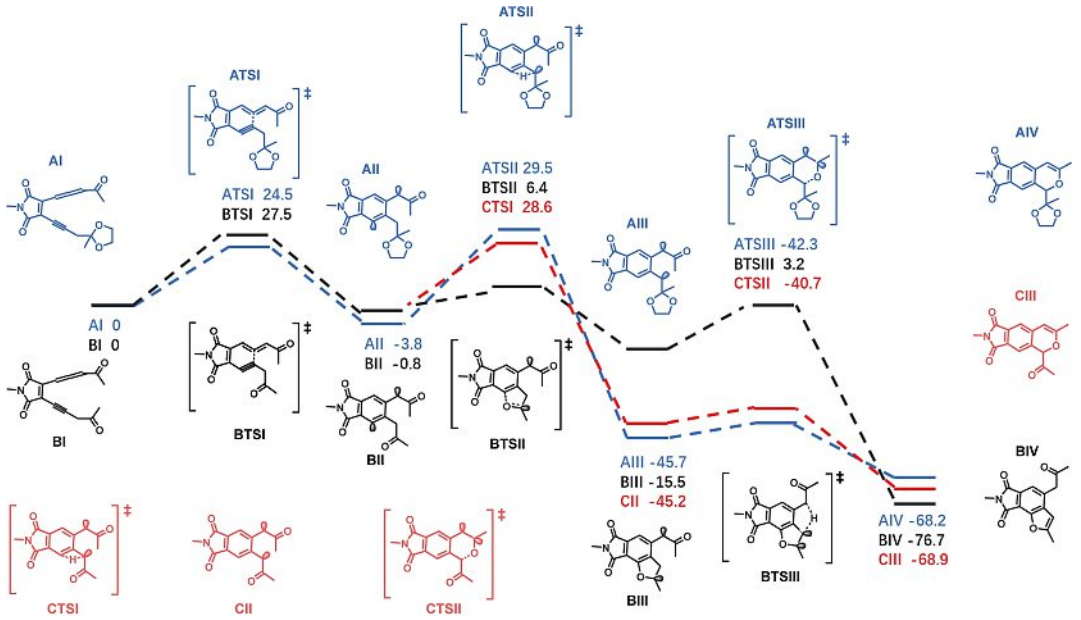

Figure 2. DFT computed Gibbs free energy profile (kcal/mol) for pathway A (blue), pathway B (black), pathway C (red).

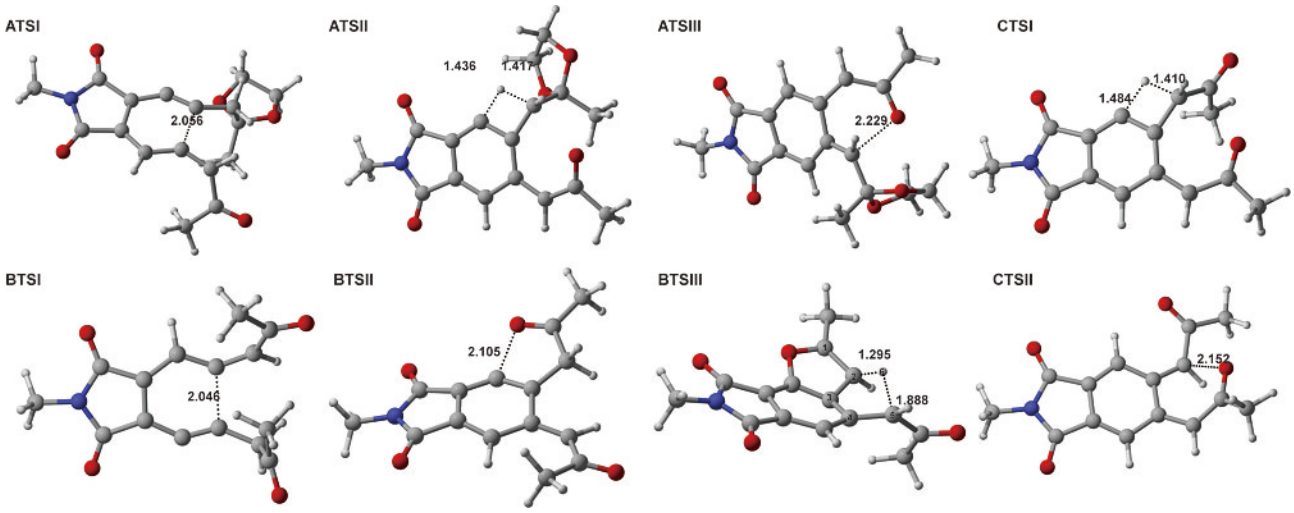

Figure 3. Optimized structures of transition states in Figure 2.

1,3-HAT/6-endo cyclization, **BII** undergoes tandem 5-endo cyclization/1,4-HAT to form **BIV**. It is worth mentioning that for **BII**, the deprotected carbonyl group provides a suitable site for phenyl radical attacking to create a five-membered ring with a more stable carbon radical and the energy barrier for this step is 7.2 kcal/mol. Moreover, the benzyl radical of diradical intermediate **BIII** transferred to the carbon atom C1 and further trapped with the radical at C2 to form the final singlet product **BIV** (Figure 3, **BTSIII**). This abnormal 1,4-HAT is accomplished via the transition state **BTSIII** with an activation energy of 18.7 kcal/mol, in which the hydrogen atom H6 together with other four atoms form a five-membered ring (C2–C5, Figure 3**, BTSIII**), and the distances of H6 to C5 and C2 are 1.888 and 1.295 Å respectively.

On the other hand, while two pathways were proposed for the formation of **CIII** (**5**): through the hydrolysis of **AIV** or the tandem 1,3-HAT/6-endo cyclization of **BII**, the result from computational calculations favors the later route. As the energy barriers are relatively low for the 6-endo cyclizations in both pathways A and C (3.4 and 4.5 kcal/mol, respectively), the 1,3-HATs turn out to be the key steps for the formation of final products and the results suggest that pathway A is less reasonable under the reaction condition with a high energy barrier of 33.3 kcal/mol for the transition state **ATSII**.

The computational results also qualitatively reflect the relative yields of pyran- and furan-type products. The energy barriers for **AII** and **BII** to undergo 1,3-HAT is 33.3 and 29.4 kcal/mol, which is less favored at room temperature, to further give pyran-type products (**4** and **5**). Therefore, the furan-type compound (**6**) dominates in the product mixture even though its precursor (**BI**) needs to be hydrolyzed from the precursor (**AI**) of pyran-type products.

To verify the reactive sites of the proposed mechanism, deuterium labeling experiment was conducted and the deuterated ratios were calculated by integration of the remaining peaks in ^{1}H NMR spectra (SI, Figure S4 and S9). The reaction was conducted under the similar condition as described above except the TFA was replaced with TFA-d. Product **5** was not isolated after the completely consumption of enediyne 1, probably due to the relatively slow hydrolysis of ketal groups in TFA-d. The deuterated sites and deuterated ratios for compound **4** and **6** are shown in Scheme 3. While in both compounds, the deuterated sites D_1 and D_2 are related to the propargyl-allene tautomerization process, D3 and D4 are possibly caused by the deuterated propargylic hydrogens or carbonyl alpha-hydrogens and the subsequent HAT.[22] It has also been observed that the methyl group in compound **4** (marked as CD_3) was deuterated for over 60% probably due to the ionization of the methyl group in TFA-d. Overall, the results of the deuterated experiments consistent with the proposed reaction pathways.

According to the above mechanistic analysis, we anticipated that if the carbonyl was protected by a more acid-sensitive group, the enyne-allene structure similar to compound **3** would yield faster, which should be more in favor of pathway B and lead to the formation of furan-type product. As acyclic acetals hydrolyze much faster than cyclic ketal groups under acidic condition,[23] an acetal-protected enediyne **7** was prepared and subjected to TFA at room temperature. The only observed product, as we expected, was the furan-type compound **8**

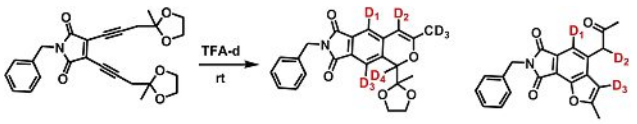

1 → 4 (12%) + 6 (37%)

	D_1	D_2	D_3	D_4
4	50%	30%	46%	12%
6	20%	36%	18%	

Scheme 3. Deuterium labeling experiment and the deuterated rates and sites for compound **4** and **6**.

(scheme 4). Compound **8** was also charicterized by ^{1}H and ^{13}NMR and HRMS (SI, Figure S9).

The understanding of the reaction pattern of the diradical intermediates from MSC provides an important guideline for the optimization of the molecular structure of enediyne as more efficient antitumor agents. As discussed above, the propargylic hydrogen atoms of enyne-allene **2** and **3** are indispensable for the HAT and the further intramolecular radical trapping which is detrimental to their DNA-cleavage ability and anticancer performance. To this end, a new asymmetric enediyne **9** (Figure 4A) was prepared, where an acid-sensitive acyclic ketal group was installed at one arm of enediyne, and tertiary butyl was equipped at the terminal of the other to block the HAT processes. Encouragingly, enediyne **9** indeed is capable of inducing DNA cleavage at low concentration (a complete disappearance of Form I is displayed in the present of 0.25 mM enediyne **9**, Figure 4C), much lower than the concentration needed for a symmetric enediyne **10** to achieve complete DNA cleavage (2 mM) (**SI**, **Scheme S1**). Moreover, enediyne **9** demonstrated an improved cytotoxicity against Hela cells compared with enediyne **10** (IC_{50} for enediyne **9** and **10** were 0.65 and 1.4 μM, respectively, Figure 4D and SI Scheme S1). The same tendency was also observed between the acetal-protected enediyne **7** and **11**, as shown in SI Scheme S1, corroborating the blocking of HAT is beneficial for improving the antitumor potency of maleimide-based enediyne antibiotics.

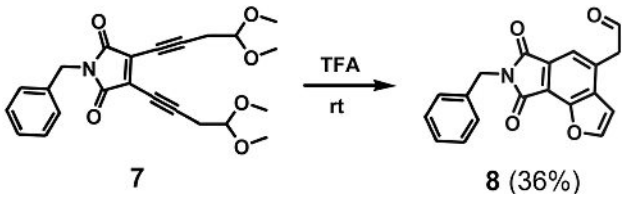

Scheme 4. The hydrolysis and cyclization of enediyne **7**.

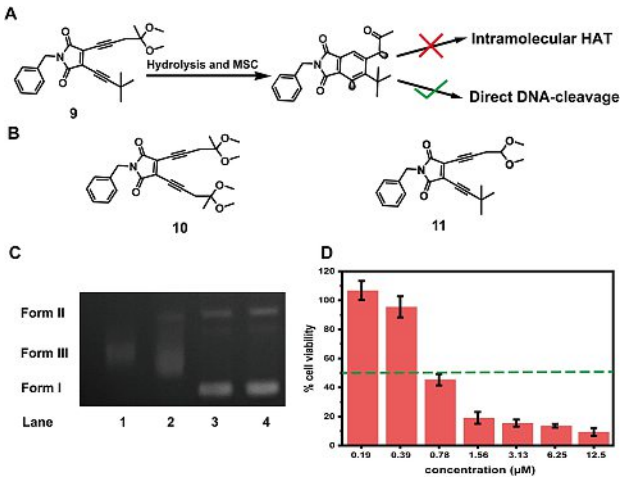

Figure 4. (A) Proposed reaction pathway for enediyne 9; (B) The structures of EDY 10 and 11. (C) DNA cleavages of enediyne 9 at pH 5.5 analyzed by gel electrophoresis technique, where Form I, Form II and Form III indicate the uncleaved native supercoiled DNA, single-strand cleaved DNA and double-strand cleaved DNA, respectively, (Lane 1: 1 mM; Lane 2: 0.25 mM; Lane 3: 0.0625 mM; Lane 4: Control); (D) In vitro cytotoxicity of enediyne 9 against HeLa cells determined by the MTT assay.

Conclusion

The reaction pathways for enediyne **1** to form intramolecular radical-quenching products were proposed according to the structural analysis of the obtained pyran- and furan-type products, which was further confirmed by DFT calculations and deuterium labeling experiment. In these pathways, enyne-allenes resulted from the hydrolysis of enediyne 1 undergo MSC to generate diradical intermediates. The subsequent 1,3-HAT/6-endo cyclization (for enyne-allene 2) or 5-endo cyclization/1,4-HAT (for enyne-allene 3) enable two radicals to be trapped into carbon-carbon double bond intramolecularly. While the energy barriers for 5-endo and 6-endo are both low, the unusual 1,4-HAT with an activation energy of 18.7 kcal/mol is preferred at room temperature over the 1,3-HAT with an activation energy of 29.4 kcal/mol, resulted in higher yield of furan-type product. Based on this mechanistic understanding, asymmetric enediyne with tertbutyl group on one end was designed to inhibit the intramolecular HAT. The newly designed enediynes demonstrated higher antitumor potency with IC_{50} value at submicromolar level, shedding light on the molecular design of acyclic enediynes as more efficient chemotherapeutic drugs.

Acknowledgements

The authors gratefully acknowledge the financial support from National Natural Science Foundation of China (21871080, 21503078), the Fundamental Research Funds for the Central Universities (22221818014), and Shanghai Leading Academic Discipline Project (B502). AH thanks the "Eastern Scholar Professorship" support from Shanghai local government. HL thanks the help from Xiaoyu Cheng.

Conflict of Interest

The authors declare no conflict of interest.

Keywords: Myers-Saito cyclization · Mechanism study · Hydrogen transfer · Intramolecular radical trapping · Antitumor agents

[1] A. G. Myers, E. Y. Kuo, N. S. Finney, *J. Am. Chem. Soc.* 1989, 111, 8057–8059.
[2] a) K. C. Nicolaou, P. Maligres, J. Shin, E. De Leon, D. Rideout, *J. Am. Chem. Soc.* **1990**, *112*, 7825–7826; b) K. C. Nicolaou, W. M. Dai, *Angew. Chem. Int. Ed. Engl.* **1991**, *30*, 1387–1416; c) L. S. Kappen, I. H. Goldberg, *Science* **1993**, *261*, 1319–1321.
[3] P. C. Dedon, Z. W. Jiang, I. H. Goldberg, *Biochemistry* **1992**, *31*, 1917–1927.
[4] a) M. Kar, A. Basak, *Chem. Rev.* **2007**, *107*, 2861–2890; b) C. Raviola, S. Protti, D. Ravelli, M. Fagnoni, *Chem. Soc. Rev.* **2016**, *45*, 4364–4390; c) K. K. Wang, *Chem. Rev.* **1996**, *96*, 207–222.

[5] a) R. Nagata, H. Yamanaka, E. Okazaki, I. Saito, *Tetrahedron Lett.* **1989**, *30*, 4995–4998; b) J. W. Grissom, D. Huang, *Angew. Chem. Int. Ed. Engl.* **1995**, *34*, 2037–2039; c) R. F. Cunico, S. K. Nair, *Tetrahedron Lett.* **1997**, *38*, 25–28; d) J. W. Grissom, D. Klingberg, D. Huang, B. J. Slattery, *J. Org. Chem.* **1997**, *62*, 603–626; e) M. Schmittel, A. A. Mahajan, G. Bucher, *J. Am. Chem. Soc.* **2005**, *127*, 5324–5325; f) M. K. Waddell, T. Bekele, M. A. Lipton, *J. Org. Chem.* **2006**, *71*, 8372–8377; g) I. Suzuki, Y. Naoe, M. Bando, H. Nemoto, M. Shibuya, *Tetrahedron Lett.* **1998**, *39*, 2361–2364.
[6] a) K. K. Wang, H.-R. Zhang, J. L. Petersen, *J. Org. Chem.* **1999**, *64*, 1650–1656; b) B. Liu, K. K. Wang, J. L. Petersen, *J. Org. Chem.* **1996**, *61*, 8503–8507; c) Y. W. Andemichael, Y. G. Gu, K. K. Wang, *J. Org. Chem.* **1992**, *57*, 794–796; d) Y. W. Andemichael, Y. Huang, K. K. Wang, *J. Org. Chem.* **1993**, *58*, 1651–1652.
[7] P. G. Dopico, M. G. Finn, *Tetrahedron* **1999**, *55*, 29–62.
[8] a) F. Ferri, R. Brückner, R. Herges, *New J. Chem.* **1998**, *22*, 531–546; b) D.-Y. Li, Y. Wei, M. Shi, *Chem. Eur. J.* **2013**, *19*, 15682–15688; c) J. Zhao, C. O. Hughes, F. D. Toste, *J. Am. Chem. Soc.* **2006**, *128*, 7436–7437; d) J. Schädlich, T. Lauterbach, M. Rudolph, F. Rominger, A. S. K. Hashmi, *J. Organomet. Chem.* **2015**, *795*, 71–77; e) Q. Y. Wang, S. Aparaj, N. G. Akhmedov, J. L. Petersen, X. D. Shi, *Org. Lett.* **2012**, *14*, 1334–1337; f) A. Basak, S. Das, D. Mallick, E. D. Jemmis, *J. Am. Chem. Soc.* **2009**, *131*, 15695–15704; g) M. Wakayama, H. Nemoto, M. Shibuya, *Tetrahedron Lett.* **1996**, *37*, 5397–5400.
[9] M. Shibuya, M. Wakayama, Y. Naoe, T. Kawakami, K. Ishigaki, H. Nemoto, H. Shimizu, Y. Nagao, *Tetrahedron Lett.* **1996**, *37*, 865–868.
[10] E. Rettenmeier, M. M. Hansmann, A. Ahrens, K. Rübenacker, T. Saboo, J. Massholder, C. Meier, M. Rudolph, F. Rominger, A. S. K. Hashmi, *Chem. Eur. J.* **2015**, *21*, 14401–14409.
[11] Y. Li, A. M. Kirillov, R. Fang, L. Yang, *Organometallics* **2017**, *36*, 1164–1172.
[12] a) D. Song, Y. Tian, S. Huang, B. Li, Y. Yuan, A. Hu, *J. Mater. Chem. B* **2015**, *3*, 8584–8588; b) D. Song, S. Sun, Y. Tian, S. Huang, Y. Ding, Y. Yuan, A. Hu, *J. Mater. Chem. B* **2015**, *3*, 3195–3200; c) J. Li, M. Zhang, S. Huang, Y. Ding, A. Hu, *Asian J. Org. Chem.* **2018**, *7*, 2076–2081; d) B. Li, M. Zhang, H. Lu, H. Ma, Y. Wang, H. Chen, Y. Ding, A. Hu, *Chem. Asian J.* **2019**, *14*, 4352–4357; e) J. Li, Y. Wu, L. Sun, S. Huang, B. Li, Y. Ding, A. Hu, *Chin. J. Chem.* **2019**, *37*, 479–485; f) Y. Wang, B. Li, M. Zhang, H. Lu, H. Chen, W. Wang, Y. Ding, A. Hu, *Tetrahedron* **2020**, *76*, 131242.
[13] M. Zhang, B. Li, H. Chen, H. Lu, H. Ma, X. Cheng, W. Wang, Y. Wang, Y. Ding, A. Hu, *J. Org. Chem.* **2020**, *85*, 9808–9819.
[14] H. Lu, H. Ma, B. Li, M. Zhang, H. Chen, Y. Wang, X. Li, Y. Ding, A. Hu, *J. Mater. Chem. B* **2020**, *8*, 1971–1979.
[15] Y. Liu, B. Yao, C.-L. Deng, R.-Y. Tang, X.-G. Zhang, J.-H. Li, *Org. Lett.* **2011**, *13*, 1126–1129.
[16] a) P. W. Peterson, R. K. Mohamed, I. V. Alabugin, *Eur. J. Org. Chem.* **2013**, 2505–2527; b) R. K. Mohamed, P. W. Peterson, I. V. Alabugin, *Chem. Rev.* **2013**, *113*, 7089–7129.
[17] a) H. Matsubara, T. Kawamoto, T. Fukuyama, I. Ryu, *Acc. Chem. Res.* **2018**, *51*, 2023–2035; b) M. Nechab, S. Mondal, M. P. Bertrand, *Chem. Eur. J.* **2014**, *20*, 16034–16059; c) M. Gulea, J. M. López-Romero, L. Fensterbank, M. Malacria, *Org. Lett.* **2000**, *2*, 2591–2594.
[18] M. J. Frisch, G. W. Trucks, H. B. Schlegel, G. E. Scuseria, M. A. Robb, J. R. Cheeseman, G. Scalmani, V. Barone, B. Mennucci, G. A. Petersson, H. Nakatsuji, M. Caricato, X. Li, H. P. Hratchian, A. F. Izmaylov, J. Bloino, G. Zheng, J. L. Sonnenberg, M. Hada, M. Ehara, K. Toyota, R. Fukuda, J. Hasegawa, M. Ishida, T. Nakajima, Y. Honda, O. Kitao, H. Nakai, T. Vreven, J. A. Montgomery, Jr., J. E. Peralta, F. Ogliaro, M. Bearpark, J. J. Heyd, E. Brothers, K. N. Kudin, V. N. Staroverov, R. Kobayashi, J. Normand, K. Raghavachari, A. Rendell, J. C. Burant, S. S. Iyengar, J. Tomasi, M. Cossi, N. Rega, J. M. Millam, M. Klene, J. E. Knox, J. B. Cross, V. Bakken, C. Adamo, J. Jaramillo, R. Gomperts, R. E. Stratmann, O. Yazyev, A. J. Austin, R. Cammi, C. Pomelli, J. W. Ochterski, R. L. Martin, K. Morokuma, V. G. Zakrzewski, G. A. Voth, P. Salvador, J. J. Dannenberg, S. Dapprich, A. D. Daniels, Ö. Farkas, J. B. Foresman, J. V. Ortiz, J. Cioslowski, D. J. Fox in *Gaussian 09, Revision E.01*,Gaussian, Inc.: Wallingford CT, **2009**.
[19] S. Grimme, J. Antony, S. Ehrlich, H. Krieg, *J. Chem. Phys.* **2010**, *132*, 154104.
[20] a) S. D. Chen, B. L. Huang, S. Y. Sun, Y. Ding, A. G. Hu, *Asian J. Org. Chem.* **2017**, *6*, 775–779; b) S. D. Chen, S. Huang, C. G. Wang, Y. Ding, A. G. Hu, *Asian J. Org. Chem.* **2017**, *6*, 1099–1103; c) T. A. Zeidan, S. V. Kovalenko, M. Manoharan, I. V. Alabugin, *J. Org. Chem.* **2006**, *71*, 962–975; d) G. Haberhauer, R. Gleiter, S. Fabig, *Org. Lett.* **2015**, *17*, 1425–1428; e) S. P. de Visser, M. Filatov, S. Shaik, *Phys. Chem. Chem. Phys.* **2001**, *3*, 1242–1245; f) B. Konig, W. Pitsch, M. Klein, R. Vasold, M. Prall, P. R. Schreiner, *J. Org. Chem.* **2001**, *66*, 1742–1746.
[21] a) T. A. Zeidan, S. V. Kovalenko, M. Manoharan, I. V. Alabugin, *J. Org. Chem.* **2006**, *71*, 962–975; b) S. Sakai, M. Nishitani, *J. Phys. Chem. A* **2010**, *114*, 11807–11813.
[22] a) H. Zhou, Y. Xing, J. Yao, J. Chen, *Org. Lett.* **2010**, *12*, 3674–3677; b) H. Zhou, D. Zhu, Y. Xie, H. Huang, K. Wang, *J. Org. Chem.* **2010**, *75*, 2706–2709.
[23] a) K. B. Wiberg, R. R. Squires, *J. Am. Chem. Soc.* **1981**, *103*, 4473–4478; b) E. H. Cordes, H. G. Bull, *Chem. Rev.* **1974**, *74*, 581–603; c) R. A. Shenoi, J. K. Narayanannair, J. L. Hamilton, B. F. L. Lai, S. Horte, R. K. Kainthan, J. P. Varghese, K. G. Rajeev, M. Manoharan, J. N. Kizhakkedathu, *J. Am. Chem. Soc.* **2012**, *134*, 14945–14957.

Manuscript received: August 10, 2020
Revised manuscript received: October 4, 2020
Accepted manuscript online: October 5, 2020
Version of record online: October 29, 2020